58. τ Branching Fractions

Revised April 2024 by Sw. Banerjee (Louisville U.) and A. Lusiani (SNS, Pisa; INFN, Pisa).

58.1 τ Branching Fractions

The τ Listings contains 252 entries that correspond to either a τ partial decay fraction into a specific decay mode (branching fraction) or a ratio of two τ partial decay fractions (branching ratio). Experimental measurements provide values for 148 of these quantities, upper limits for 67 branching fractions to Lepton Family number, Lepton number, or Baryon number violating modes, and 37 additional upper limits for other modes. A total of 129 τ branching fractions and branching ratios are determined with a fit of 170 measurements. 85 quantities have at least one measurement in the fit.

58.2 The constrained fit to τ branching fractions

The τ branching fractions fit uses the reported values, uncertanties and statistical correlations of the τ branching fractions and branching ratios measurements. Asymmetric uncertainties are symmetrized as $\sigma^2_{\rm symm} = (\sigma^2_+ + \sigma^2_-)/2$. If only a few measurements are correlated, the correlation coefficients are listed in the footnote for each measurement (see for example Γ(particle$^-$ $\geq$ 0 neutrals $\geq 0\,K^0 \nu_\tau$ ("1-prong"))/$\Gamma_{\rm total}$). If a large number of measurements are correlated, then the full correlation matrix is listed in the footnote to the measurement that first appears in the τ Listings. Footnotes to the other measurements refer to the first one. For example, the large correlation matrices for the branching fraction or ratio measurements contained in Refs. [1] [2] are listed in Footnotes to the $\Gamma(e^-\overline{\nu}_e\nu_\tau)/\Gamma_{\rm total}$ and $\Gamma(h^-\nu_\tau)/\Gamma_{\rm total}$ measurements respectively. Additionally, the most precise experimental inputs are treated according to how they depend on external parameters on the basis of their documentation [3]. The τ measurements may depend on parameters such as the τ pair production cross-section in e^+e^- annihilations at the $\Upsilon(4S)$ peak. In some cases, measurements reported in different papers by the same collaboration may depend on common parameters like the estimate of the integrated luminosity or of particle identification efficiencies. For all the significant detected dependencies, the τ measurements and their uncertainties are updated to account for the updated values of the external parameters. The dependencies on common systematic effects are also determined in size and sign, and all the common systematic dependencies of different measurements are used together with the published statistical and systematic uncertainties and correlations in order to compute an updated all-inclusive variance and covariance matrix of the experimental inputs of the fit.

The fit procedure parameters correspond to all measured τ branching fractions and ratios, to some non-measured branching fractions and ratios like for instance $\mathcal{B}(\tau^- \to \pi^- K^0_L K^0_L \nu_\tau)$ and to one nuisance variable. When discussing the fit results in the following, the fit χ^2, the number of degrees of freedom, the residuals and pulls all refer to the subset of fit parameters that correspond to τ branching fractions and ratios, excluding nuisance variables. The fit parameters are optimized while respecting relations described by a series of constraint equations. All the experimental inputs and all the constraint equations are reported in the τ Listings section that follows this review. In some cases, constraints describe approximate relations that nevertheless hold within the present experimental precision. For instance, the constraint $\mathcal{B}(\tau^- \to K^-K^-K^+\nu_\tau) = \mathcal{B}(\tau^- \to K^-\phi\nu_\tau) \times \mathrm{B}(\phi \to K^+K^-)$ is justified within the current experimental evidence. The constraint equations between the τ branching fractions and ratios include quantities other than τ branching fractions and branching ratios, like for instance the branching fractions of the η and ω mesons. We neglect the uncertainties on these values for all quantities except $\mathcal{B}(a_1^- \to \pi^-\gamma)$, whose value and uncertainty were estimated by ALEPH [1] to be $(0.21 \pm 0.08)\cdot 10^{-2}$, relying on a measurement of $\Gamma(a_1^- \to$

$\pi^-\gamma$) [4]. This quantity is included in the fit parameters as nuisance variable, with a χ^2 term corresponding to its estimate. We assume that $\mathcal{B}(\tau^- \to a_1^- \nu_\tau) = \mathcal{B}(\tau^- \to \pi^-\pi^+\pi^-\nu_\tau \text{ (ex.}K^0, \omega)) + \mathcal{B}(\tau^- \to \pi^- 2\pi^0 \nu_\tau \text{ (ex.}K^0)) + \mathcal{B}(\tau^- \to a_1^-(\pi^-\gamma)\nu_\tau)$, neglecting the observed but negligible branching fractions to other modes, and that $\mathcal{B}(\tau^- \to a_1^-(\pi^-\gamma)\nu_\tau) = \mathcal{B}(\tau^- \to a_1^-\nu_\tau) \cdot \mathcal{B}(a_1^- \to \pi^-\gamma)$. The values of all other quantities in the constraint equations are taken from the 2023 edition of the Review of Particle Physics.

In the fit, uncertainty scale factors are applied to the published uncertainties of measurements only if significant inconsistency between different measurements remain after accounting for all relevant uncertainties and correlations. When performing the fit with no scale factors, the two measurements of $\mathcal{B}(\tau^- \to K^-K^-K^+\nu_\tau)$ have pulls exceeding $5\,\sigma$ from the fit values. There are 170 pulls, one per measurement. They are partially correlated, and the effective number of independent pulls is equal to the number of degrees of freedom of the fit, 125. The probability of getting pulls equal or larger than either one of the two very large pulls in a sample of 125 is smaller that the probability of a $3\,\sigma$ deviation for a Normal variable. Therefore, it has been decided to apply an uncertainty scale factor of 5.4 on all measurements of $\mathcal{B}(\tau^- \to K^-K^-K^+\nu_\tau)$ (one by BaBar and one by Belle). The scale factor has been computed according to the standard PDG procedure. After applying the scale factor, the pull distribution of the measurements in figure 58.1 is reasonably Normal and the pull probability distribution in figure 58.2 is reasonably flat.

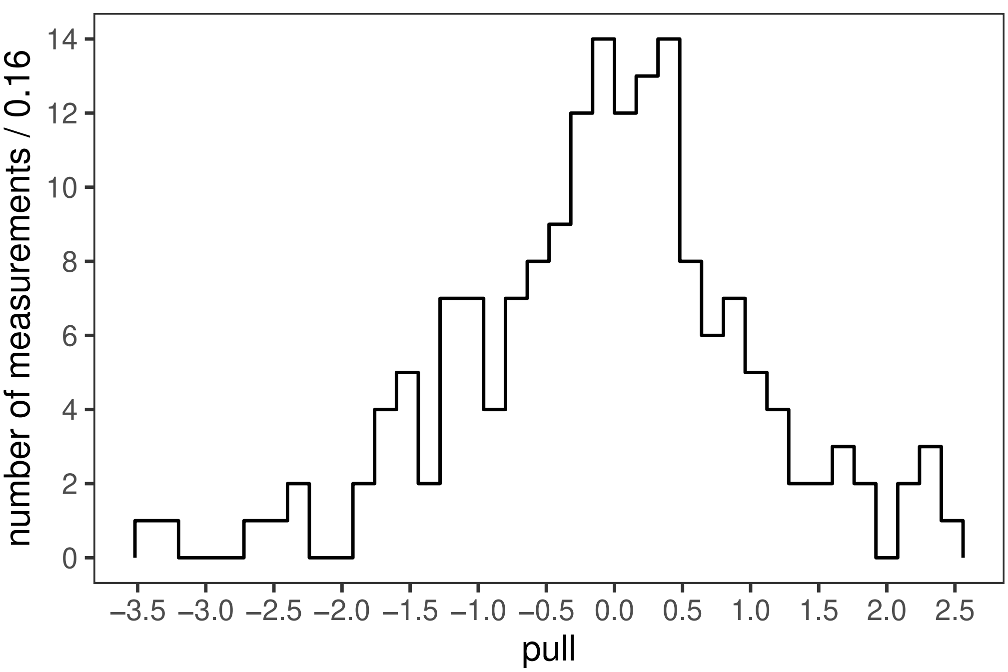

Figure 58.1: Pulls of individual measurements against the respective fitted quantity.

Considering only the residuals with respect to τ branching fractions and ratios measurements, the constrained fit has a χ^2 of 135 for 125 degrees of freedom, corresponding to a χ^2 probability of 26.0%. We use 170 measurements and 84 constraints on the branching fractions and ratios to determine 129 quantities, consisting of 112 branching fractions and 17 branching ratios. The constraints include the unitarity constraint on the sum of all the exclusive τ decay modes, $\mathcal{B}_{\text{all}} = 1$. If the unitarity constraint is released, the fit result for $\mathcal{B}_{\text{all}}$ is consistent with unitarity with $1 - \mathcal{B}_{\text{all}} = (0.07 \pm 0.11)\%$.

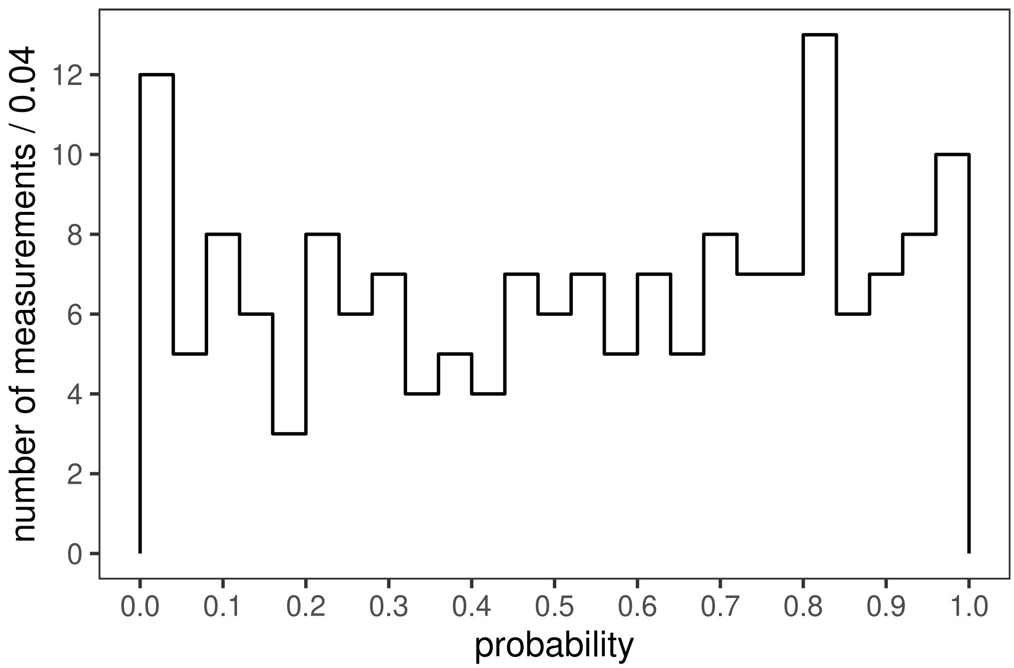

Figure 58.2: Probability of individual measurement pulls against the respective fitted quantity.

For the convenience of summarizing the fit results, we list in the following the values and uncertainties for a set of 46 "basis" decay modes, from which all remaining branching fractions and ratios can be obtained using the constraints. The basis decay modes are not intended to sum up to 1. Since some basis quantities represent multiple branching fractions that are related by constraint equations, the unitarity constraint corresponds to a linear combination of branching fractions, with the coefficients listed in the following. The coefficients of $\mathcal{B}(\tau^- \to \pi^- 2\pi^0 \nu_\tau \text{ (ex.} K^0))$ and $\mathcal{B}(\tau^- \to \pi^-\pi^+\pi^-\nu_\tau \text{ (ex.} K^0, \omega))$ depend on the fitted value of the nuisance variable, $\mathcal{B}(a_1^- \to \pi^-\gamma) = 0.0022 \pm 0.0008$. The correlation matrix between the basis modes is reported in the τ Listings.

In defining the fit constraints and in selecting the modes that sum up to one we made some assumptions and choices. We assume that some channels, like $\tau^- \to \pi^- K^+ \pi^- \geq 0\pi^0 \nu_\tau$ and $\tau^- \to \pi^+ K^- K^- \geq 0\pi^0 \nu_\tau$, have negligible branching fractions as expected from the Standard Model, even if the experimental limits for these branching fractions are not very stringent. The 95% confidence level upper limits are $\mathcal{B}(\tau^- \to \pi^- K^+ \pi^- \geq 0\pi^0 \nu_\tau) < 0.25\%$ and $\mathcal{B}(\tau^- \to \pi^+ K^- K^- \geq 0\pi^0 \nu_\tau) < 0.09\%$, values not so different from measured branching fractions for allowed 3-prong modes containing charged kaons. For decays to final states containing one neutral kaon we assume that the branching fraction with the K_L^0 are the same as the corresponding one with a K_S^0. On decays with two neutral kaons we assume that the branching fractions with $K_L^0 K_L^0$ are the same as the ones with $K_S^0 K_S^0$.

58.3 BaBar and Belle measure on average lower branching fractions and ratios.

We compare the BaBar and Belle measurements with the results of a fit where all the B-factories measurements have been excluded. We restrict the comparison to the measurements that are used in the fit, omitting two measurements that are superseeded with other results, and one measurement that is fully correlated with other measurements. We find that BaBar and Belle measure on average lower τ branching fractions and ratios than the other experiments. Figures 58.3 and 58.4 show

decay mode	fit result	coefficient
$\mathcal{B}(\tau^- \to \mu^- \bar{\nu}_\mu \nu_\tau)$	0.1739 ± 0.0004	1.0000
$\mathcal{B}(\tau^- \to e^- \bar{\nu}_e \nu_\tau)$	0.1782 ± 0.0004	1.0000
$\mathcal{B}(\tau^- \to \pi^- \nu_\tau)$	0.1082 ± 0.0005	1.0000
$\mathcal{B}(\tau^- \to K^- \nu_\tau)$	0.00696 ± 0.00010	1.0000
$\mathcal{B}(\tau^- \to \pi^- \pi^0 \nu_\tau)$	0.2549 ± 0.0009	1.0000
$\mathcal{B}(\tau^- \to K^- \pi^0 \nu_\tau)$	0.00433 ± 0.00015	1.0000
$\mathcal{B}(\tau^- \to \pi^- 2\pi^0 \nu_\tau \text{ (ex.}K^0))$	0.0926 ± 0.0010	1.0022
$\mathcal{B}(\tau^- \to K^- 2\pi^0 \nu_\tau \text{ (ex.}K^0))$	$(0.65 \pm 0.22) \cdot 10^{-3}$	1.0000
$\mathcal{B}(\tau^- \to \pi^- 3\pi^0 \nu_\tau \text{ (ex.}K^0))$	0.0104 ± 0.0007	1.0000
$\mathcal{B}(\tau^- \to K^- 3\pi^0 \nu_\tau \text{ (ex.}K^0, \eta))$	$(0.48 \pm 0.21) \cdot 10^{-3}$	1.0000
$\mathcal{B}(\tau^- \to h^- 4\pi^0 \nu_\tau \text{ (ex.}K^0, \eta))$	0.0011 ± 0.0004	1.0000
$\mathcal{B}(\tau^- \to \pi^- \bar{K}^0 \nu_\tau)$	0.00838 ± 0.00014	1.0000
$\mathcal{B}(\tau^- \to K^- K^0 \nu_\tau)$	0.001486 ± 0.000034	1.0000
$\mathcal{B}(\tau^- \to \pi^- \bar{K}^0 \pi^0 \nu_\tau)$	0.00382 ± 0.00013	1.0000
$\mathcal{B}(\tau^- \to K^- K^0 \pi^0 \nu_\tau)$	0.00150 ± 0.00007	1.0000
$\mathcal{B}(\tau^- \to \pi^- \bar{K}^0 2\pi^0 \nu_\tau \text{ (ex.}K^0))$	$(0.26 \pm 0.23) \cdot 10^{-3}$	1.0000
$\mathcal{B}(\tau^- \to \pi^- K_S^0 K_S^0 \nu_\tau)$	$(235 \pm 6) \cdot 10^{-6}$	2.0000
$\mathcal{B}(\tau^- \to \pi^- K_S^0 K_L^0 \nu_\tau)$	0.00108 ± 0.00024	1.0000
$\mathcal{B}(\tau^- \to \pi^- K_S^0 K_S^0 \pi^0 \nu_\tau)$	$(18.2 \pm 2.1) \cdot 10^{-6}$	2.0000
$\mathcal{B}(\tau^- \to \pi^- K_S^0 K_L^0 \pi^0 \nu_\tau)$	$(0.32 \pm 0.12) \cdot 10^{-3}$	1.0000
$\mathcal{B}(\tau^- \to \bar{K}^0 h^- h^- h^+ \nu_\tau)$	$(0.25 \pm 0.20) \cdot 10^{-3}$	1.0000
$\mathcal{B}(\tau^- \to \pi^- \pi^+ \pi^- \nu_\tau \text{ (ex.}K^0, \omega))$	0.0899 ± 0.0005	1.0022
$\mathcal{B}(\tau^- \to \pi^- \pi^+ \pi^- \pi^0 \nu_\tau \text{ (ex.}K^0, \omega))$	0.0274 ± 0.0007	1.0000
$\mathcal{B}(\tau^- \to h^- h^- h^+ 2\pi^0 \nu_\tau \text{ (ex.}K^0, \omega, \eta))$	0.0010 ± 0.0004	1.0000
$\mathcal{B}(\tau^- \to \pi^- K^- K^+ \nu_\tau)$	0.001435 ± 0.000027	1.0000
$\mathcal{B}(\tau^- \to \pi^- K^- K^+ \pi^0 \nu_\tau)$	$(61 \pm 18) \cdot 10^{-6}$	1.0000
$\mathcal{B}(\tau^- \to \pi^- \pi^0 \eta \nu_\tau)$	0.00139 ± 0.00007	1.0000
$\mathcal{B}(\tau^- \to K^- \eta \nu_\tau)$	$(155 \pm 8) \cdot 10^{-6}$	1.0000
$\mathcal{B}(\tau^- \to K^- \pi^0 \eta \nu_\tau)$	$(48 \pm 12) \cdot 10^{-6}$	1.0000
$\mathcal{B}(\tau^- \to \pi^- \bar{K}^0 \eta \nu_\tau)$	$(94 \pm 15) \cdot 10^{-6}$	1.0000
$\mathcal{B}(\tau^- \to \pi^- \pi^+ \pi^- \eta \nu_\tau \text{ (ex.}K^0))$	$(220 \pm 13) \cdot 10^{-6}$	1.0000
$\mathcal{B}(\tau^- \to K^- \omega \nu_\tau)$	$(0.41 \pm 0.09) \cdot 10^{-3}$	1.0000
$\mathcal{B}(\tau^- \to h^- \pi^0 \omega \nu_\tau)$	0.0041 ± 0.0004	1.0000
$\mathcal{B}(\tau^- \to K^- \phi \nu_\tau)$	$(44 \pm 16) \cdot 10^{-6}$	0.8300
$\mathcal{B}(\tau^- \to \pi^- \omega \nu_\tau)$	0.0195 ± 0.0006	1.0000
$\mathcal{B}(\tau^- \to K^- \pi^- \pi^+ \nu_\tau \text{ (ex.}K^0, \omega))$	0.00293 ± 0.00007	1.0000
$\mathcal{B}(\tau^- \to K^- \pi^- \pi^+ \pi^0 \nu_\tau \text{ (ex.}K^0, \omega, \eta))$	$(0.39 \pm 0.14) \cdot 10^{-3}$	1.0000
$\mathcal{B}(\tau^- \to \pi^- 2\pi^0 \omega \nu_\tau)$	$(72 \pm 16) \cdot 10^{-6}$	1.0000
$\mathcal{B}(\tau^- \to 2\pi^- \pi^+ 3\pi^0 \nu_\tau \text{ (ex.}K^0, \eta, \omega, f_1))$	$(14 \pm 27) \cdot 10^{-6}$	1.0000
$\mathcal{B}(\tau^- \to 3\pi^- 2\pi^+ \nu_\tau \text{ (ex.}K^0, \omega, f_1))$	$(775 \pm 30) \cdot 10^{-6}$	1.0000
$\mathcal{B}(\tau^- \to K^- 2\pi^- 2\pi^+ \nu_\tau \text{ (ex.}K^0))$	$(0.6 \pm 1.2) \cdot 10^{-6}$	1.0000
$\mathcal{B}(\tau^- \to 2\pi^- \pi^+ \omega \nu_\tau \text{ (ex.}K^0))$	$(84 \pm 6) \cdot 10^{-6}$	1.0000
$\mathcal{B}(\tau^- \to 3\pi^- 2\pi^+ \pi^0 \nu_\tau \text{ (ex.}K^0, \eta, \omega, f_1))$	$(38 \pm 9) \cdot 10^{-6}$	1.0000
$\mathcal{B}(\tau^- \to K^- 2\pi^- 2\pi^+ \pi^0 \nu_\tau \text{ (ex.}K^0))$	$(1.1 \pm 0.6) \cdot 10^{-6}$	1.0000
$\mathcal{B}(\tau^- \to \pi^- f_1 (2\pi^- 2\pi^+) \nu_\tau)$	$(52 \pm 4) \cdot 10^{-6}$	1.0000
$\mathcal{B}(\tau^- \to \pi^- 2\pi^0 \eta \nu_\tau \text{ (ex.}K^0))$	$(0.19 \pm 0.04) \cdot 10^{-3}$	1.0000

histograms of the 25 pulls of the differences between B-factory measurements and the respective non-B-factory fit results. The average pull between the two sets of measurements is -0.8σ (-0.7σ for the 14 Belle measurements and -0.9σ for the 11 BaBar measurements).

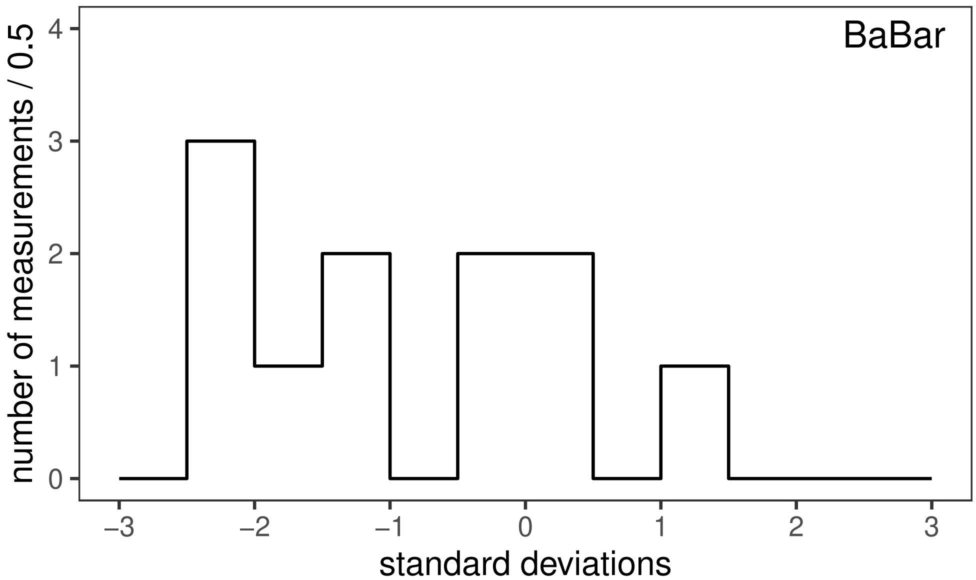

Figure 58.3: Distribution of the normalized difference between 11 measurements of branching fractions and ratios published by the BaBar collaboration and the respective averages computed using only non-B-factory measurements.

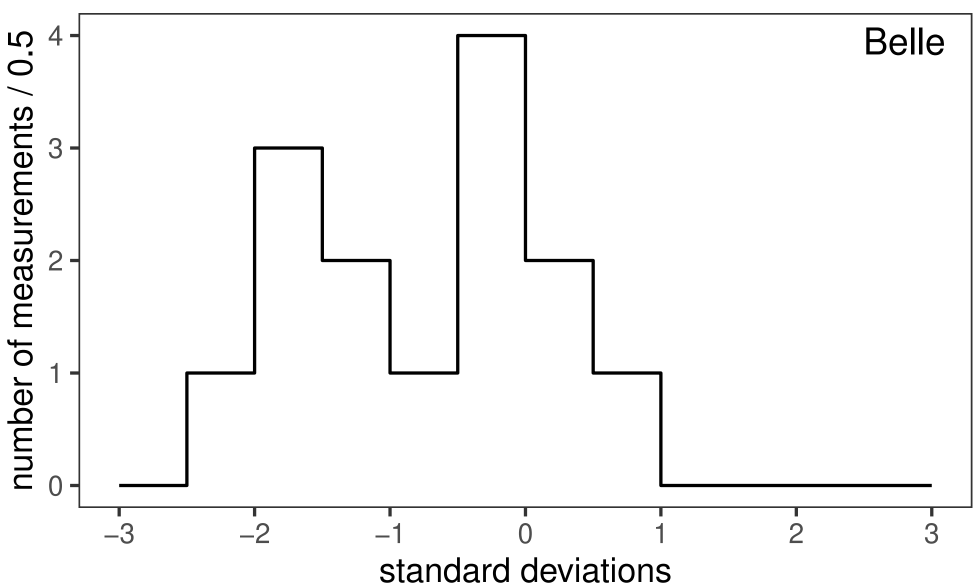

Figure 58.4: Distribution of the normalized difference between 14 measurements of branching fractions and ratios published by the Belle collaboration and the respective averages computed using only non-B-factory measurements.

58.4 Overconsistency of Leptonic Branching Fraction Measurements.

As observed in the previous editions of this review, measurements of the leptonic branching fractions are more consistent with each other than expected from the quoted uncertainties on the individual measurements. The χ^2/n.d.o.f. are 0.34/4 for $\mathcal{B}_e$ and 0.08/4 for $\mathcal{B}_\mu$. The probability of getting a smaller χ^2 is 1.3% for B_e and 0.08% for B_μ.

58.5 Technical implementation of the fit

The fit computes a set of quantities denoted with q_i by minimizing a χ^2 while respecting a series of equality constraints on the q_i. The quantities q_i represent τ branching fractions and branching ratios, and nuisance variables. The fit minimization procedure is equivalent to choosing a set of basis fit variables, using functions of these basis variables to predict measurements, and determining these basis variables by minimizing the measurements' χ^2. The χ^2 is computed using the measurements m_i and their covariance matrix E_{ij} as $\chi^2 = (m_i - A_{ik}q_k)^t E_{ij}^{-1}(m_j - A_{jl}q_l)$, where the model matrix A_{ij} is used to get the vector of the predicted measurements m'_i from the vector of the fit parameters q_j as $m'_i = A_{ij}q_j$. There is one fit variable for each of the modes that have measurements, therefore $A_{ij} = 1$ when q_j corresponds to the τ branching fraction or branching ratio of the measurement m_i, and $A_{ij} = 0$ otherwise. The constraints are equations involving the fit parameters. The fit does not impose limitations on the functional form of the constraints. In summary, the fit requires:

$$\min\left[\chi^2(q_k)\right] = \min\left[(m_i - A_{ik}q_k)^t E_{ij}^{-1}(m_j - A_{jl}q_l)\right] \ , \tag{58.1}$$

$$\text{subjected to} \quad f_r(q_s) - c_r = 0 \ , \tag{58.2}$$

where the left term of Eq. 58.2 defines the constraint expressions. Using the method of Lagrange multipliers, a set of equations is obtained by taking the derivatives with respect to the fitted quantities q_k and the Lagrange multipliers λ_r of the sum of the χ^2 and the constraint expressions multiplied by the Lagrange multipliers λ_r, one for each constraint:

$$\begin{aligned} \min\left[(A_{ik}q_k - m_i)^t E_{ij}^{-1}(A_{jl}q_l - m_j) + 2\lambda_r(f_r(q_s) - c_r)\right] &= \\ = \min\left[\tilde{\chi}^2(q_k, \lambda_r)\right] \ , & \\ (\partial/\partial q_k, \partial/\partial\lambda_r)\left[\tilde{\chi}^2(q_k, \lambda_r)\right] = 0 \ . & \end{aligned} \tag{58.3}$$

Eq. 58.3 defines a set of equations for the vector of the unknowns (q_k, λ_r), some of which may be non-linear, in case of non-linear constraints. An iterative minimization procedure approximates at each step the non-linear constraint expressions by their first order Taylor expansion around the current values of the fitted quantities, $\bar{q}_s$:

$$f_r(q_s) - c_r = f_r(\bar{q}_s) + \left.\frac{\partial f_r(q_s)}{\partial q_s}\right|_{\bar{q}_s} (q_s - \bar{q}_s) - c_r \ ,$$

which can be written as

$$B_{rs}q_s - c'_r \ ,$$

where c'_r are the resulting constant known terms, independent of q_s at first order. After linearization, the differentiation by q_k and λ_r is trivial and leads to a set of linear equations

$$A_{ki}^t E_{ij}^{-1} A_{jl} q_l + B_{kr}^t \lambda_r = A_{ki}^t E_{ij}^{-1} m_j \ , \tag{58.4}$$

$$B_{rs}q_s = c'_r \ , \tag{58.5}$$

which can be expressed as

$$F_{ij} u_j = v_i \ , \tag{58.6}$$

where $u_j = (q_k, \lambda_r)$ and v_i is the vector of the known constant terms running over the index k and then r in the right terms of Eq. 58.4 and Eq. 58.5, respectively. Solving the equation set in Eq. 58.6 by matrix inversion gives the the fitted quantities and their variance and covariance matrix, using the measurements and their variance and covariance matrix. The fit procedure starts by computing the linear approximation of the non-linear constraint expressions around the quantities seed values. With an iterative procedure, the unknowns are updated at each step by solving the equations and the equations are then linearized around the updated values, until the variation of the fitted unknowns is reduced below a numerically small threshold.

References

[1] S. Schael *et al.* (ALEPH), Phys. Rept. **421**, 191 (2005), [hep-ex/0506072].

[2] J. Abdallah *et al.* (DELPHI), Eur. Phys. J. **C46**, 1 (2006), [hep-ex/0603044].

[3] D. Asner *et al.* (Heavy Flavor Averaging Group) (2010), [arXiv:1010.1589].

[4] M. Zielinski *et al.*, Phys. Rev. Lett. **52**, 1195 (1984).